Combustion Theory and Modelling
Vol. 12, No. 6, 2008, 1179–1196

Taylor & Francis
Taylor & Francis Group

A theoretical study of spontaneous ignition of fuel jets in an oxidizing ambient with emphasis on hydrogen jets

K.B. Lim[a], B.H. Chao[b*], P.B. Sunderland[a], and R.L. Axelbaum[c]

[a]*Department of Fire Protection Engineering, University of Maryland, College Park, MD 20742, USA;*
[b]*Department of Mechanical Engineering, University of Hawaii at Manoa, Honolulu, HI 96822, USA;*
[c]*Department of Energy, Environmental and Chemical Engineering, Washington University, St. Louis, MO 63130, USA*

(*Received 4 October 2007; final version received 23 April 2008*)

An analysis was performed for the spontaneous ignition of a hydrogen (or other gaseous fuel) jet emanating from a slot into an oxidizing ambient (e.g., air). A similarity solution of the flow field was obtained. This was combined with the species and energy conservation equations, which were solved using activation energy asymptotics. Limits of spontaneous ignition were identified as functions of slot width, flow rate, and temperatures of the hydrogen jet and ambient gas. Two scenarios are examined: a cool jet flowing into a hot ambient and a hot jet flowing into a cool ambient. For both scenarios, ignition is favored with an increase of either the ambient temperature or the hydrogen supply temperature. Moreover, for the hot ambient scenario, a decrease in fuel Lewis number also promotes ignition. The Lewis number of the oxidizer only has a weak effect on ignition. Because spontaneous ignition is very sensitive to temperature, ignition is expected to occur near the edge of the jet if the hydrogen is cooler than the ambient gas and near the centerline if the hydrogen is hotter than the ambient gas.

Keywords: Spontaneous ignition; Hydrogen jets; Activation energy asymptotics; Lewis numbers; Ignition location

Nomenclature

a_T	constant representing the temperature increase through reaction
a_F	constant representing the fuel consumption through reaction
B	pre-exponential factor
c_p	specific heat at constant pressure
D	mass diffusion coefficient
Da	Damköhler number
$\tilde{D}a$	reduced Damköhler number
$\bar{D}a$	rescaled reduced Damköhler number defined in Eq. (44)
E	activation temperature
f	nondimensional streamfunction
h	half width of the slot
Le	Lewis number
n	reaction order

*Corresponding author. E-mail: bchao@eng.hawaii.edu

ISSN: 1364-7830 print / 1741-3559 online

DOI: 10.1080/13647830802315095
http://www.tandf.co.uk/journals

p pressure
Pr Prandtl number
q_F heat of combustion per unit mass of fuel
R ideal gas constant
Sc Schmidt number
T temperature
$\hat{T}$ reference temperature
u flow velocity in the x (streamwise) direction
v flow velocity in the y (transverse) direction
W molecular weight
x streamwise spatial coordinate
x_0 distance from the virtual origin of the jet to the exit of the slot
y transverse spatial coordinate ($y = 0$ along the centerline)
Y mass fraction
Z mixture fraction

Greek symbols

α parameter defined as $\alpha = (\tilde{T}_\infty - \tilde{T}_0)/\tilde{Y}_{F,0}$
β parameter defined as $\beta = (\tilde{T}_0 - \tilde{T}_\infty)/\tilde{Y}_{O,\infty}$
ε small parameter used for asymptotic expansion
ϕ perturbation of species concentration in the reaction region
θ perturbation of temperature in the reaction region
λ thermal conductivity
μ viscosity
ν stoichiometric coefficient
ρ gas density
ψ streamfunction
η similarity variable
σ stoichiometric oxidizer to fuel mass ratio
ξ stretched spatial coordinate in the reaction region along the streamwise direction for the hot jet scenario
ζ stretched spatial coordinate in the reaction region along the transverse direction

Subscripts

0 value of variables at the exit of the slot
F fuel
f frozen solution
I ignition state
O oxidizer
∞ ambient condition

Superscripts

$\sim$ nondimensional quantity
$\wedge$ rescaled nondimensional quantity based on $\hat{T}$

1. Introduction

Concerns about the emissions of greenhouse gases and supply of oil have led to extensive consideration of hydrogen as a major fuel carrier. Nonetheless, hydrogen presents several unusual fire hazards, including high leak propensity, ease of ignition, and invisible flames. For example, heated air jets flowing into hydrogen will ignite spontaneously at an air temperature of 913 K [1]. This is cooler than for other fuels [1, 2], including gasoline and methane, and is not much higher than the autoignition temperature of stoichiometric hydrogen/air mixtures, 858 K [3]. Occasional unintended hydrogen leaks will be unavoidable, and some may involve heated hydrogen and/or air. Thus an improved understanding of limits of spontaneous ignition of hydrogen jets is sought here, with the aid of activation-energy asymptotics.

Zheng and Law [4] identified ignition limits of premixed hydrogen–air flames where ignition was by a heated counterflowing stream. The ignition limits of non-premixed hydrogen–air jets will be different from those of premixed counterflowing streams because of the non-premixed nature and the absence of strain due to counterflow heating.

Thermal ignition in subsonic [5] and supersonic [6, 7] mixing layers has been studied by activation energy asymptotics and numerically with one-step reaction as well as reduced mechanisms. Im et al. [6] employed a reduced mechanism to analyze thermal ignition in a supersonic hydrogen/air mixing layer and obtained ignition characteristics over a wide range of conditions. These findings are particularly applicable to scramjets. Lee and Chung [8] investigated the different combustion regimes in a stagnant mixing layer by employing Damköhler-number and activation-energy asymptotics, based on an eight-step reduced mechanism. Law and co-workers [9, 10] investigated the ignition of hydrogen and air in a mixing layer by using reduced reaction mechanisms that they developed.

Toro et al. [11] examined in detail the structure of laminar hydrogen jet flames both experimentally and numerically. Chaos et al. [12] examined Lewis-number effects in unsteady laminar hydrogen jet flames, which will have different effects compared to steady laminar hydrogen jet flames. Liu and Pei [13] examined autoignition and explosion limits of hydrogen–oxygen mixtures in homogeneous systems, which involved reduced mechanisms. Dryer et al. [14] examined spontaneous ignition of pressurized releases of hydrogen and natural gas into air. This investigation involved multi-dimensional transient flows with shock formation, reflection and interactions that resulted in the transition to turbulent jet nonpremixed combustion. This is a different aspect of risk, associated with rapid failures of pressure vessels, as compared to the scenario being considered here, which involves small leaks/cracks that are undetected, and that ignite spontaneously when the limits are reached.

The present study applies asymptotic analysis to investigate the spontaneous ignition of a laminar jet of hydrogen, or another gaseous fuel, leaking through a crack into an oxidizing ambient. Asymptotic flame theories can provide valuable insights into combustion reactions [15–18]. Quantitative and predictive derivations can be made using the concept of distinguished limits in activation energy asymptotics. Based largely on the concept of Zel'dovich number, asymptotic analysis enables evaluation of temperature effects on reaction rates despite the narrowness of the reaction zone relative to the transport zones of the flame structure.

The crack is taken to be straight and long, yielding a two-dimensional flow field. The ignition analysis identifies limits of spontaneous ignition. Unfortunately, comparisons with experiments are not possible because no study to date of spontaneous ignition of nonpremixed jets has measured the key phenomena analyzed here.

The objectives of this work are to: (1) develop a model of spontaneous ignition for two cases: a cool fuel jet flowing into heated ambient gas and a heated fuel jet flowing into cool ambient gas; (2) identify limits of spontaneous ignition as functions of slot width, flow rate, fuel Lewis

number, and temperatures of the fuel jet and the ambient gas; and (3) identify the location of ignition.

2. Formulation

The problem of interest is a steady, isobaric laminar jet of fuel (e.g. hydrogen) at temperature T_0 issuing from a rectangular slot into an oxidizing environment (e.g. atmospheric air) at a temperature of T_∞, as shown schematically in Figure 1. Spontaneous ignition occurs when either T_0 or T_∞ is sufficiently high that the weak reaction between the fuel and the oxidizer transitions to a vigorous burning flame. This study analyzes the ignition state as a function of various physical properties including Lewis number, T_0, T_∞, the flow velocity at the slot exit, u_0, and the width of the slot. The slot is considered sufficiently long that end effects are negligible. The reaction chemistry is assumed to follow a single-step, overall, irreversible reaction with second order Arrhenius kinetics and a high activation energy.

With the above problem definition, conservation of mass and momentum are given by

$$\frac{\partial(\rho u)}{\partial x} + \frac{\partial(\rho v)}{\partial y} = 0, \tag{1}$$

$$\rho u \frac{\partial u}{\partial x} + \rho v \frac{\partial u}{\partial y} - \frac{\partial}{\partial y}\left(\mu \frac{\partial u}{\partial y}\right) = 0, \tag{2}$$

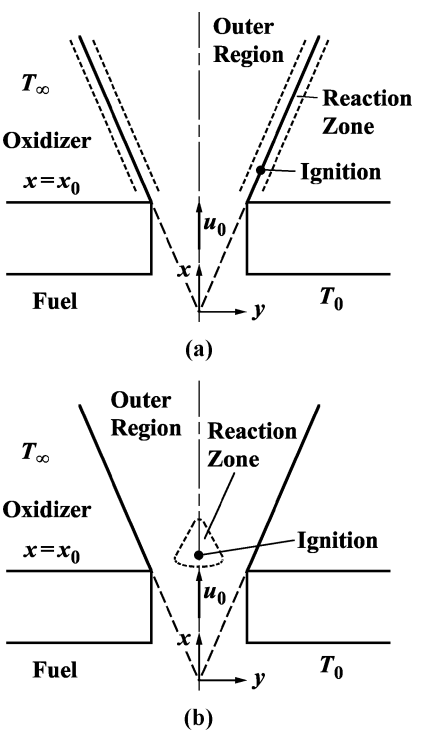

Figure 1. Schematic of slot and fuel (e.g. hydrogen) leak for the (a) hot ambient and (b) hot jet cases.

which are to be solved subject to the boundary conditions

$$y = 0,\ x = x_0 :\ u = u_0,\ v = 0;\ x > x_0 :\ \partial u/\partial y = 0,\ v = 0, \tag{3}$$

$$y \to \infty : u \to 0. \tag{4}$$

Introducing a streamfunction ψ of the form

$$\rho u = \rho_\infty u_0 (\partial \psi/\partial y),\ \rho v = -\rho_\infty u_0 (\partial \psi/\partial x), \tag{5}$$

such that Eq. (1) is satisfied, transforming the coordinates from (x, y) to $(\tilde{x}, \eta)$ where

$$\tilde{x} = x/x_0,\ \eta = [\rho_\infty u_0/(6\mu_\infty x_0)]^{1/2} \tilde{x}^{-2/3} \int_0^y (\rho/\rho_\infty) dy, \tag{6}$$

and defining

$$\psi = [6\mu_\infty x_0/(\rho_\infty u_0)]^{1/2} \tilde{x}^{1/3} f(\eta), \tag{7}$$

Equations (2)–(4) are transformed to

$$(f'''/2) + f f'' + f'^2 = 0, \tag{8}$$

$$\eta = 0: f = f'' = 0,\ f' = 1;\ \eta \to \infty :\ f' \to 0. \tag{9}$$

The notations used in this study are listed in the Nomenclature section. A similarity solution is assumed to exist so that f is a function of η only. Solving Equations (8)–(9) following Bickey [19] and Schlichting [20] yields $f = \tanh \eta$. In these equations, x_0 is the value of x at the slot exit from the virtual origin of the jet, which can be determined by the conservation of the x-momentum across the slot exit, given by

$$x_0 = 3\rho_0^2 \left[\int_{-h}^{h} (u_{x=x_0^-})^2 dy \right]^2 / \left(32 u_0^3 \rho_\infty \mu_\infty\right). \tag{10}$$

Applying the coordinate transformation and the solution of the momentum equation to the energy and species conservation equations, we obtain

$$\frac{1}{Pr} \frac{\partial^2 \tilde{T}}{\partial \eta^2} + 2(\tanh \eta) \frac{\partial \tilde{T}}{\partial \eta} - 6(\operatorname{sech}^2 \eta) \tilde{x} \frac{\partial \tilde{T}}{\partial \tilde{x}} = -Da\, \tilde{x}^{4/3} \tilde{Y}_F \tilde{Y}_O \tilde{T}^{-1} \exp(-\tilde{E}/\tilde{T}), \tag{11}$$

$$\frac{1}{Sc_F} \frac{\partial^2 \tilde{Y}_F}{\partial \eta^2} + 2(\tanh \eta) \frac{\partial \tilde{Y}_F}{\partial \eta} - 6(\operatorname{sech}^2 \eta) \tilde{x} \frac{\partial \tilde{Y}_F}{\partial \tilde{x}} = Da\, \tilde{x}^{4/3} \tilde{Y}_F \tilde{Y}_O \tilde{T}^{-1} \exp(-\tilde{E}/\tilde{T}), \tag{12}$$

$$\frac{1}{Sc_O} \frac{\partial^2 \tilde{Y}_O}{\partial \eta^2} + 2(\tanh \eta) \frac{\partial \tilde{Y}_O}{\partial \eta} - 6(\operatorname{sech}^2 \eta) \tilde{x} \frac{\partial \tilde{Y}_O}{\partial \tilde{x}} = Da\, \tilde{x}^{4/3} \tilde{Y}_F \tilde{Y}_O \tilde{T}^{-1} \exp(-\tilde{E}/\tilde{T}), \tag{13}$$

which are to be solved subject to

$$\eta = 0, \tilde{x} = 1 : \quad \tilde{T} = \tilde{T}_0, \quad \tilde{Y}_F = \tilde{Y}_{F,0}, \quad \tilde{Y}_O = 0, \tag{14}$$

$$\eta = 0,\ \tilde{x} > 1 : \quad \partial \tilde{T}/\partial \eta = \partial \tilde{Y}_F/\partial \eta = \partial \tilde{Y}_O/\partial \eta = 0, \tag{15}$$

$$\eta \to \infty : \quad \tilde{T} \to \tilde{T}_\infty, \quad \tilde{Y}_F \to 0, \quad \tilde{Y}_O \to \tilde{Y}_{O,\infty}. \tag{16}$$

In the above,

$$\tilde{T} = \frac{c_p\, T}{q_F},\ \tilde{Y}_F = Y_F,\ \tilde{Y}_O = \frac{Y_O}{\sigma},\ Da = \frac{6\, x_0\, \nu_O\, c_p\, p\, B}{W_F\, q_F\, R\, u_0},\ \tilde{E} = \frac{c_p\, E}{q_F},$$
$$Pr = \frac{\mu}{\lambda/c_p},\ Sc_j = \frac{\mu}{\rho\, D_j},\ Le_j = \frac{\lambda/c_p}{\rho\, D_j},\ \sigma = \frac{\nu_O\, W_O}{\nu_F\, W_F}.$$

The values of c_p, $\rho\,\lambda$, $\rho\,\mu$, and $\rho^2 D_j$ are considered constant. The ideal gas equation of state has been adopted in the derivation of Equations (11)–(13).

In the non-reactive limit, solving Equations (11)–(13), but without the reaction terms, subject to Equations (14)–(16) gives the frozen solutions,

$$\tilde{T}_f = \tilde{T}_\infty + (\tilde{T}_0 - \tilde{T}_\infty)\,(\operatorname{sech}^{2\,Pr}\eta)\,/\,\tilde{x}^{1/3}, \tag{17}$$
$$\tilde{Y}_{F,f} = \tilde{Y}_{F,0}\,(\operatorname{sech}^{2\,Sc_F}\eta)/\tilde{x}^{1/3}, \tag{18}$$
$$\tilde{Y}_{O,f} = \tilde{Y}_{O,\infty}\,[1 - (\operatorname{sech}^{2\,Sc_O}\eta)/\tilde{x}^{1/3}]. \tag{19}$$

2.1. *Cool jet flowing into a hot ambient ($T_\infty > T_0$)*

In the presence of a weak reaction, the temperature is increased from its frozen value by a small, $O(\varepsilon)$ amount where $\varepsilon = \tilde{T}_\infty^2/\tilde{E}$ while the reactant concentrations are reduced from their respective frozen values by an $O(\varepsilon)$ amount. Because of the high activation energy, ignition is primarily controlled by temperature and occurs near $\eta \to \infty$ if successful. Away from this high temperature region, the reaction is negligible and can be considered frozen. In the outer, chemically frozen region, the solutions are similar to Equations (17)–(19) but with an $O(\varepsilon)$ change in their values. With the application of Equations (14) and (15), the solutions of $\tilde{T}$ and $\tilde{Y}_F$ are given by

$$\tilde{T} = (\tilde{T}_\infty + \varepsilon\, a_T) - [(\tilde{T}_\infty - \tilde{T}_0) + \varepsilon\, a_T]\,(\operatorname{sech}^{2\,Pr}\eta)\,/\,\tilde{x}^{1/3} + O(\varepsilon^2), \tag{20}$$
$$\tilde{Y}_F = \varepsilon\, a_F + (\tilde{Y}_{F,0} - \varepsilon\, a_F)\,(\operatorname{sech}^{2\,Sc_F}\eta)\,/\,\tilde{x}^{1/3} + O(\varepsilon^2). \tag{21}$$

The solution of $\tilde{Y}_O$ is not important to the analysis.

In the inner, reactive region, a stretched spatial inner variable is defined as

$$\zeta = \tilde{Y}_{F,0}\,(\operatorname{sech}\eta)^{2Pr}/(\varepsilon\,\tilde{x}^{1/3}), \tag{22}$$

while the solutions are expanded as

$$\tilde{T} = \tilde{T}_\infty + \varepsilon\,(\theta - \alpha\,\zeta) + O(\varepsilon^2), \tag{23}$$
$$\tilde{Y}_F = \varepsilon^{Le_F}\,(\tilde{Y}_{F,0}/\tilde{x}^{1/3})^{1-Le_F}\,\zeta^{Le_F} + O(\varepsilon), \tag{24}$$
$$\tilde{Y}_O = \tilde{Y}_{O,\infty} + O(\varepsilon). \tag{25}$$

Equation (24) is obtained by considering Le_F to be sufficiently smaller than unity, as for hydrogen. Substitution of Equations (22)–(25) into Equation (11) and expanding in orders of ε yield

$$\zeta^2\,(\partial^2\theta/\partial\,\zeta^2) = -\,\tilde{D}a\,\zeta^{Le_F}\,\exp(\theta - \alpha\,\zeta), \tag{26}$$

where $\alpha = (\tilde{T}_\infty - \tilde{T}_0)/\tilde{Y}_{F,0}$ is the parameter indicating the effect of temperature difference and $\tilde{Da}$ is the reduced Damköhler number defined as

$$\tilde{Da} = Da\,\tilde{Y}_{O,\infty}\,\tilde{x}^{4/3}\,[\,\tilde{Y}_{F,0}/(\varepsilon\,\tilde{x}^{1/3})\,]^{1-Le_F}\,\exp(-\tilde{E}/\tilde{T}_\infty)/(4\,Pr\,\tilde{T}_\infty). \tag{27}$$

The boundary conditions required to solve this equation can be found by applying Equations (22) and (23) to Equation (16), and matching the inner and outer solutions to yield

$$\zeta = 0: \theta = 0;\ \zeta \to \infty:\ \partial\theta/\partial\zeta \to 0,\ \theta \to a_T. \tag{28}$$

For the case of Le_F close to unity, as for most of gaseous fuels, Equation (24) is modified to

$$\tilde{Y}_F = \varepsilon\,(\phi_F + \zeta) + O(\varepsilon^2), \tag{29}$$

Substitution of Equations (22), (23), (25) and (29) into Equations (11) and (12) gives

$$\zeta^2(\partial^2\theta/\partial\zeta^2) = -\tilde{Da}\,(\phi_F + \zeta)\exp(\theta - \alpha\zeta), \tag{30}$$

$$\partial^2(\theta + \phi_F)/\partial\zeta^2 = 0, \tag{31}$$

where $\tilde{Da}$ is given by Equation (27) with $Le_F = 1$. Applying the boundary conditions of Equation (16) and the conditions obtained by matching the inner and outer solutions as before, we obtain Equation (28) and $\phi_F = -\theta$, which can be applied to Equation (30) to yield

$$\zeta^2(\partial^2\theta/\partial\zeta^2) = -\tilde{Da}\,(\zeta - \theta)\exp(\theta - \alpha\zeta). \tag{32}$$

2.2. *Hot jet flowing into a cool ambient ($T_0 > T_\infty$)*

For the case of a hot jet issuing into a cold ambient, any ignition will occur near the jet centerline, $\eta = 0$. Moreover, because the jet will be cooled by the cold ambient gas along the flow, ignition is expected to occur near the slot exit. The analysis is similar to that in Section 2.1, except that $\varepsilon = \tilde{T}_0^2/\tilde{E}$, the inner spatial variables are defined as

$$\zeta = \eta\,(Pr\,\tilde{Y}_{O,\infty}/\varepsilon)^{1/2}, \quad \xi = \tilde{Y}_{O,\infty}\,(\tilde{x} - 1)/(3\,\varepsilon), \tag{33}$$

and the inner solutions are expanded as

$$\tilde{T} = \tilde{T}_0 + \varepsilon\,[\theta - \beta\,(\zeta^2 + \xi)] + O(\varepsilon^2), \tag{34}$$

$$\tilde{Y}_F = \tilde{Y}_{F,0} + O(\varepsilon), \tag{35}$$

$$\tilde{Y}_O = \varepsilon\,(\phi_O + Le_O\,\zeta^2 + \xi) + O(\varepsilon^2). \tag{36}$$

Substitution of Equations (33)–(36) into Equations (11) and (13) leads to

$$\frac{\partial^2\theta}{\partial\zeta^2} - 2\frac{\partial\theta}{\partial\xi} + \frac{1}{Le_O}\frac{\partial^2\phi_O}{\partial\zeta^2} - 2\frac{\partial\phi_O}{\partial\xi} = 0, \tag{37}$$

$$\frac{\partial^2\theta}{\partial\zeta^2} - 2\frac{\partial\theta}{\partial\xi} = -\tilde{Da}\,(\phi_O + Le_O\,\zeta^2 + \xi)\exp[\theta - \beta(\zeta^2 + \xi)], \tag{38}$$

with the initial and boundary conditions

$$\xi = 0: \theta = \phi_O = 0, \tag{39}$$

$$\zeta = 0 \text{ and } \zeta \to \infty,\ \xi > 0: \partial\theta/\partial\zeta = \partial\phi_O/\partial\zeta = 0, \tag{40}$$

where $\beta = (\tilde{T}_0 - \tilde{T}_\infty)/\tilde{Y}_{O,\infty}$ and $\tilde{Da}$ is

$$\tilde{Da} = \varepsilon\,[Da\,\tilde{Y}_{F,0}/(\tilde{T}_0\,\tilde{Y}_{O,\infty})]\,\exp(-\tilde{E}/\tilde{T}_0). \tag{41}$$

Ignition is considered successful when the heat generation through reaction is sufficient to compensate for the heat loss from the jet to the ambient at any location, i.e. when the reaction is self-sustainable. The ignition criterion is then defined as

$$(\partial\theta/\partial\xi)_{\zeta=0} \geq \beta \textit{ or } \partial\theta/\partial\zeta \geq 2\beta\zeta \text{ at any } \xi. \tag{42}$$

The smallest value of ξ that satisfies either of these conditions represents the first point that thermal runaway would occur and is identified as the location of ignition.

3. Results and Discussion

3.1. *Cool jet flowing into a hot ambient ($T_\infty > T_0$)*

For this case, Equation (26) subject to Equation (28) was solved by a fourth order Runge-Kutta method. The results are shown in Figure 2, a plot of the reaction temperature increase, a_T, versus reduced Damköhler number, $\tilde{Da}$, for selected values of $\alpha = (\tilde{T}_\infty - \tilde{T}_0)/\tilde{Y}_{F,0}$ and $Le_F = 0.6$. This reveals the lower and middle branches of an S-shaped ignition/extinction curve [3,15,16]. In each such curve, there is a maximum value of $\tilde{Da}$ above which a solution does not exist. For values of $\tilde{Da}$ smaller than this critical value, there are two solutions for each $\tilde{Da}$. The critical value of $\tilde{Da}$ represents the transition from weak reaction to vigorous burning, and is defined as the ignition state, $\tilde{Da}_I$. The lower branch, showing an increase of temperature with higher reaction rate, is the physically realistic branch. The middle branch represents conditions that are not physically possible. Spontaneous ignition is successful for any $\tilde{Da}$ greater than $\tilde{Da}_I$.

Figure 2 indicates that a decrease in α reduces $\tilde{Da}_I$, which means that ignition is favored. Such a decrease can be accomplished by increasing the jet temperature, $\tilde{T}_0$, q_F/c_p. For these cases, reaction is enhanced when α is reduced such that it is easier to ignite the reactants. A fuel such as hydrogen (which has q_F/c_p of roughly 78 600 K in air), is hence more ignitable as compared to fuels such as methane ($q_F/c_p = 36\,800$ K) and isooctane ($q_F/c_p = 33\,800$ K) when the flow conditions are the same. As an example, for $Y_{F,0}=1$, $T_0 = 300$ K and $T_\infty = 1000$ K, the values of α are 0.0089, 0.019 and 0.021 for hydrogen, methane and isooctane, respectively.

Parameter α also can be changed by variations in the ambient temperature, $\tilde{T}_\infty$, or the reactant mass fraction in the fuel supply, $\tilde{Y}_{F,0}$, but these changes result in a simultaneous change of $\tilde{Da}$ as can be seen from Equation (27). To investigate the effects of $\tilde{T}_\infty$ at fixed $\tilde{Da}$, a rescaling is required. The rescaling is performed by specifying a reference value of $\tilde{T}_\infty$ as $\hat{T}_\infty$, defining rescaled parameters $\hat{\varepsilon} = \hat{T}_\infty^2/\tilde{E}$, $\hat{a}_T = (\tilde{T}_\infty/\hat{T}_\infty)^2\,a_T$ and

$$\hat{Da} = Da\,\tilde{Y}_{O,\infty}\,\tilde{x}^{4/3}\,[\tilde{Y}_{F,0}/(\hat{\varepsilon}\,\tilde{x}^{1/3})]^{(1-Le_F)}\,\exp(-\tilde{E}/\hat{T}_\infty)/(4\,Pr\,\hat{T}_\infty). \tag{43}$$

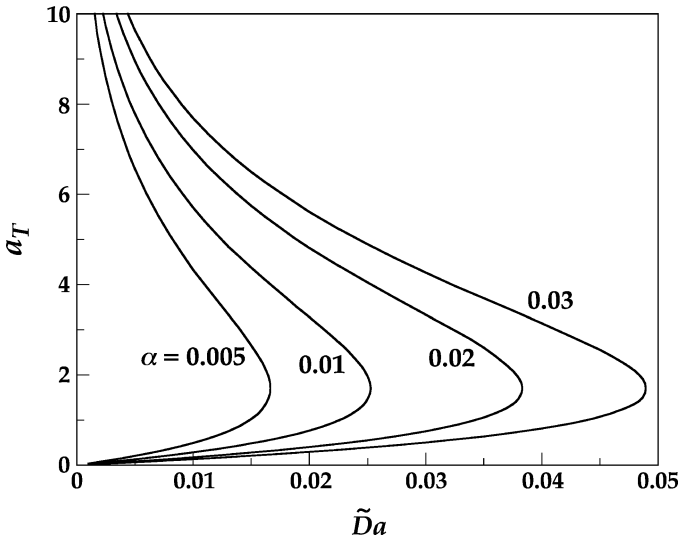

Figure 2. Reaction temperature increase a_T versus reduced Damköhler number $\tilde{D}a$ for selected values of $\alpha = (\tilde{T}_\infty - \tilde{T}_0)/\tilde{Y}_{F,0}$ with $Le_F = 0.6$. The plot is for a cool jet flowing into a hot ambient.

and plotting the results in terms of rescaled variables $\hat{a}_T$ and $\hat{D}a$. In this section, $\tilde{T}_0 = 0.00382$, $\tilde{E} = 0.127$, $\tilde{Y}_{F,0} = 1$ and $\hat{T}_\infty = 0.01382$ were used to exhibit the ignition behavior. These data correspond to $T_0 = 300$ K, $E = 10\,000$ K, $T_{\infty,ref} = 1090$ K for hydrogen. The rescaled results are shown in Figure 3. Here an increase in $\tilde{T}_\infty$, which increases α without changing $\hat{D}a$, is seen to favor ignition. This also is physically realistic because more heat is transferred to the cold fuel

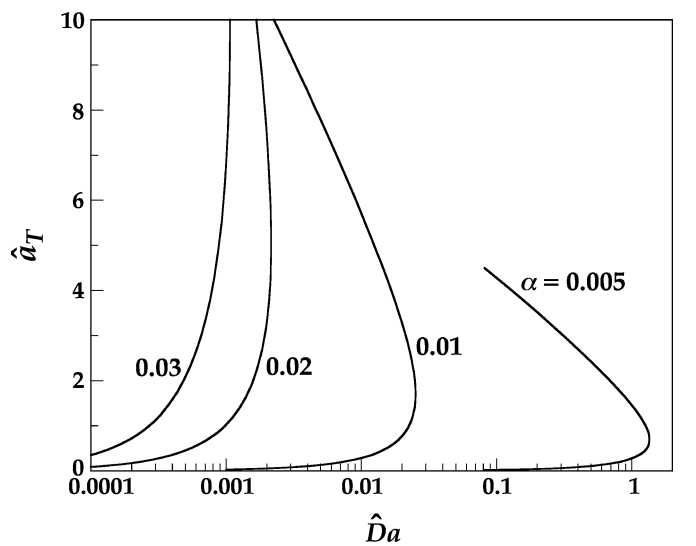

Figure 3. Rescaled plot of $\hat{a}_T$ versus $\hat{D}a$ from Figure 2 when changes of α is caused by variations in $\tilde{T}_\infty$, with $\tilde{T}_0 = 0.00382$, $\tilde{E} = 0.127$, $\tilde{Y}_{F,0} = 1$, and $\hat{T}_\infty = 0.01382$.

flow at a higher rate when the ambient is at a higher temperature. For the same reason, when the kinetic data are unchanged, an increased $\tilde{T}_\infty$ yields ignition closer to the exit of the slot. Note that the reduced Damköhler number shown in Equation (27) is a function of the axial distance from the virtual origin of the jet.

When the variation of α is caused by the change of $\tilde{Y}_{F,0}$, a similar rescaling of $\tilde{D}a$ by defining a reference value of $\tilde{Y}_{F,0}$ is necessary. The result is qualitatively the same as that presented in Figure 2, which is expected because an increase in $\tilde{Y}_{F,0}$ (a decrease in α) results in a greater fuel concentration in the reaction region and a higher reaction rate.

To investigate the influence of fuel Lewis number, Le_F, on ignition, a reference fuel Lewis number is necessary. As can be seen after Equation (16), Le_F is defined as the mixture thermal diffusivity divided by the mass diffusivity of fuel into the mixture. Specifying $Le_F = 1$ as the reference Le_F, we define a second rescaled reduced Damköhler number from Equation (43) as

$$\bar{D}a = Da\, \tilde{Y}_{O,\infty}\, \tilde{x}^{4/3}\, \exp(-\tilde{E}/\hat{T}_\infty)/(4\, Pr\, \hat{T}_\infty). \tag{44}$$

The results for $\alpha = 0.02$ are presented in Figure 4 by plotting a_T versus $\bar{D}a$. The curve for $Le_F = 1$ was obtained by solving Equation (32) subject to Equation (28). For demonstration purpose, a value of $\tilde{x} = 2$ also is specified whenever Equation (44) is used. Only quantitative differences exist when another value of $\tilde{x}$ is adopted. Figure 4 shows that a decrease in Le_F for fixed $\bar{D}a$ favors ignition. This occurs because a smaller Le_F implies that fuel species diffuse more quickly into the hot oxidizer. A fuel such as hydrogen, which has Le_F of 0.6 or less in mixtures of nitrogen, is hence more ignitable as compared to fuels such as isooctane and methane, which have higher Le_F, under the same conditions. Nayagam and Williams [21] found that in a one-dimensional model of steady motion of edges of reaction sheets, increasing the Lewis number decreases the propagation velocity at small Damköhler numbers. This indicates that the reaction rate is raised when Le_F is reduced, which agrees with the findings of Figure 4.

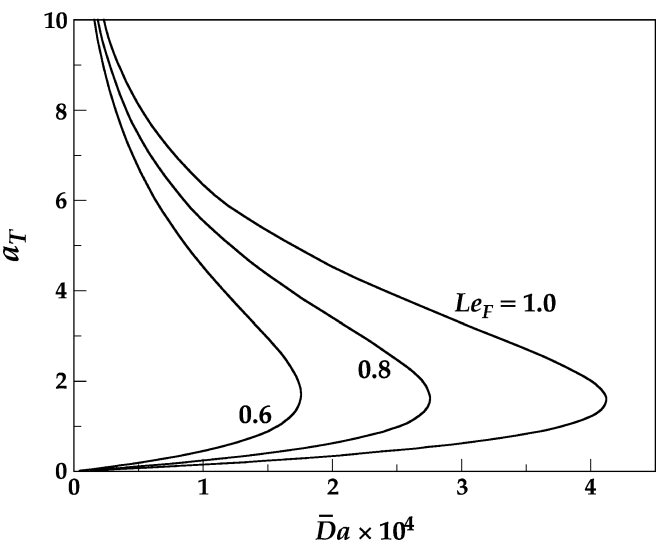

Figure 4. Reaction temperature increase a_T versus reduced Damköhler number $\bar{D}a$ for selected values of Le_F, with $\alpha = 0.02$, and $\tilde{x} = 2$, cool jet flowing into hot ambient.

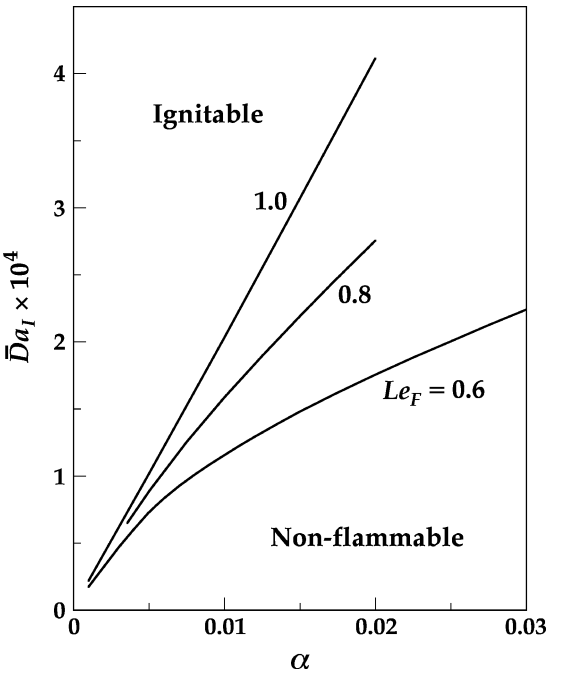

Figure 5. Variation of the ignition state, $\bar{D}a_I$, versus α (which is changed by variations in $\tilde{T}_0$) for selected values of Le_F, with $\tilde{E}= 0.127$, $\hat{T}_\infty= 0.01382$, $\tilde{x}= 2$ and $\tilde{T}_\infty = 0.02382$, cool jet flowing into hot ambient.

The ignition states for the three values of Le_F adopted in Figure 4 are shown in Figure 5 by plotting the reduced Damköhler number at ignition, $\bar{D}a_I$, versus α with fixed $\tilde{T}_\infty= 0.02382$. Although the selection of $\tilde{T}_\infty$ may be quantitatively unrealistic for values of α greater than 0.02, the proper qualitative behavior is exhibited. The value is chosen such that Figures 4 and 5 are plotted using the same parameters. The region above the curve for any Le_F is the region in which ignition is successful and a flame can be established while the region below the curve is the region where ignition fails. The plot shows that ignition is favored when α is decreased since $\bar{D}a_I$ is reduced, as discussed earlier. Moreover, as Le_F is decreased, the ignitable region is broadened such that ignition occurs more easily. This figure again shows that hydrogen is more diffusive and, hence, more ignitable (more dangerous from a fire safety perspective) than other hydrocarbon fuels, which is consistent with the findings shown in Figure 4.

For cases where the variation of α is caused by a change of $\tilde{T}_\infty$, the ignition state is presented in Figure 6, which shows that ignition is favored for larger α and smaller Le_F, as was seen in Figures 3–5. The effect of the reaction order of the fuel, which can be obtained by replacing $\tilde{Y}_F$ with $\tilde{Y}_F^{n_F}$ in the reaction term of Equations (11)–(13), also has been studied. The results show that ignition is favored when the reaction order is increased because of an increased reaction rate. Its effect, however, is much weaker as compared to other effects already discussed.

3.2. *Hot jet flowing into a cool ambient ($T_0 > T_\infty$)*

For this scenario, ignition is expected to occur near the centerline because the fuel is hotter than the ambient gas. To obtain the ignition condition, Equations (37)–(40) were solved by the Crank-Nicholson method and the resulting matrix was inverted by LU decomposition. The solution of

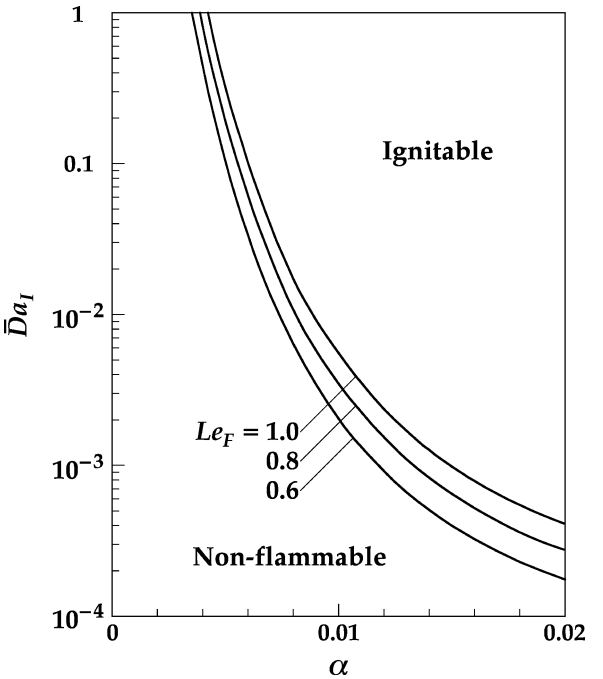

Figure 6. Variation of the ignition state, $\bar{D}a_I$, versus α corresponding to Figure 5 when changes of α is caused by variations in $\tilde{T}_\infty$.

θ, the temperature increase through reaction, is plotted versus ζ in Figure 7 for selected values of ξ. Here $\beta = 0.3$, $\tilde{D}a = 0.5$ and $Le_O = 1$, where $\beta = (\tilde{T}_0 - \tilde{T}_\infty)/\tilde{Y}_{O,\infty}$ and $\tilde{D}a$ is given by Equation (41). At the jet exit, $\xi = 0$, there is no reaction so $\theta = 0$. With the increase of ξ, reaction takes place and θ increases. For this case, a maximum θ is developed away from but close to the centerline of the jet, $\zeta = 0$. Although the reaction is very sensitive to temperature variations, it also needs the oxidizer. When moving away from $\zeta = 0$, the temperature reduces while the oxidizer concentration increases. The maximum value of θ then is located where the maximum reaction rate occurs through the competition of these two effects. At $\xi = 1.153$, the reaction is sufficiently strong and the heat generation is sufficiently high to overcome the heat loss to the cold ambient such that one of the conditions in Equation (42) is satisfied and ignition is successful. The value of $\xi = 1.153$ is then identified as the ignition location ξ_I and the maximum value of θ at ξ_I is defined as $\theta_{\max}$. Beyond $\xi_I = 1.153$, θ continues to increase, reaches a maximum value, and then gradually drops to 0 as $\xi \to \infty$. That is, the temperature continues to increase, reaches its maximum, and decreases to T_∞ as $\xi \to \infty$. Thermal runaway is not observed because of the strong heat loss from the reaction region to the ambient, given by the $\exp[-\beta(\zeta^2 + \xi)]$ term of Equation (38). This part of the solution is unrealistic because once ignition is successful at ξ_I, a flame is established and the weak-reactive assumption is no longer valid. It is expected that thermal runaway would be predicted by a transient analysis of the temporal evolution of temperature at $\xi_I = 1.153$.

If ignition fails, $(\partial\theta/\partial\xi)_{\zeta=0}$ first increases and then decreases such that $(\partial\theta/\partial\xi)_{\zeta=0} \geq \beta$ can never be satisfied, because the heat generation is not high enough to overcome the heat loss to the ambient. For smaller values of $\tilde{D}a$ (but still large enough to yield ignition), $\theta_{\max}$ is established away from $\zeta = 0$ in the beginning, and later shifts to the centerline before ignition occurs. The

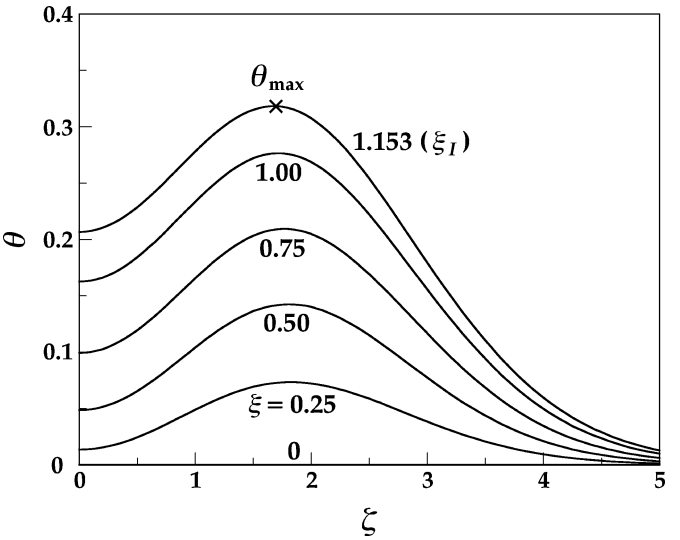

Figure 7. Evolution of the temperature increase through reaction, θ, versus ζ for some values of ξ until ignition. The plot is for a hot jet flowing into a cool ambient with $\beta = 0.3$, $\tilde{Da} = 0.5$ and $Le_O = 1$.

reason for this is that the values of ξ_I are relatively large and sufficient oxidizer is transported to the centerline such that ignition is dominated by the high temperature at the centerline.

Results of ignition conditions for three values of β are shown in Figures 8 and 9 by plotting $\theta_{\max}$ and ξ_I, respectively, versus $\tilde{Da}$ for $Le_O = 1$. On each curve, by increasing the reaction rate, i.e. $\tilde{Da}$, a smaller temperature increase and a shorter ignition location are observed before ignition. A higher value of $\tilde{Da}$ yields an increased heat generation rate, which further compensates for heat loss from the hot jet to the cold ambient and favors ignition. The stronger reaction rate

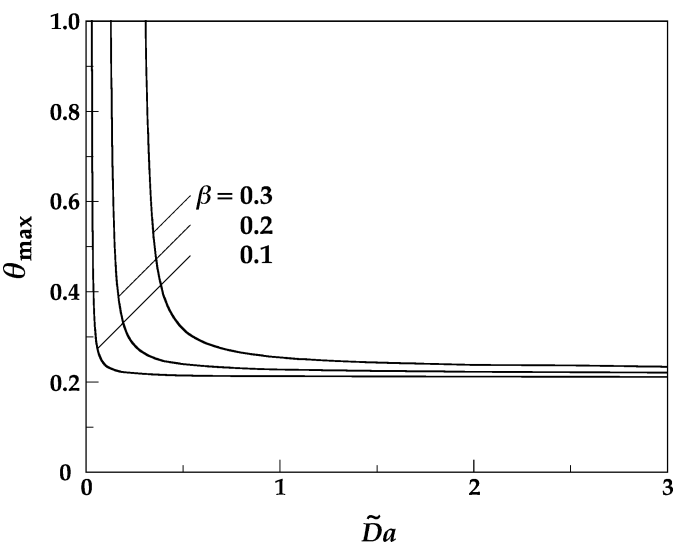

Figure 8. Reaction temperature increase before ignition, $\theta_{\max}$, versus reduced Damköhler number $\tilde{Da}$ for selected values of $\beta = (\tilde{T}_0 - \tilde{T}_\infty)/\tilde{Y}_{O,\infty}$ and $Le_O = 1$, hot jet flowing into cool ambient.

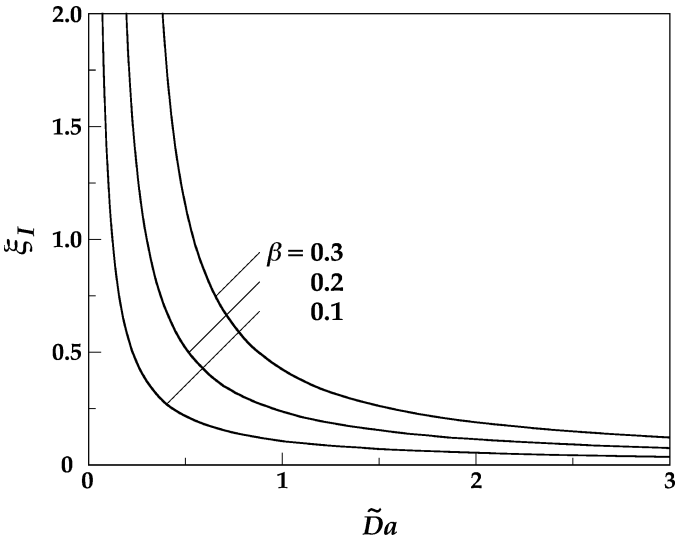

Figure 9. Ignition location ξ_I corresponding to Figure 8.

also brings the point of ignition closer to the jet exit. In contrast, a reduction in $\tilde{Da}$ weakens the reaction and makes ignition more difficult such that both $\theta_{\max}$ and ξ_I increase. Although an increase of ξ provides longer residence time for the reaction so that ignition can occur at a smaller $\tilde{Da}$, the reaction rate decreases with ξ because the jet is cooled by the cold ambient, as can be seen from the reaction term of Equation (38). A sharp increase in $\theta_{\max}$ and ξ_I for lower values of $\tilde{Da}$ on each β curve in Figures 8 and 9 means that the reduction of reaction rate dominates over the residence time increase, and defines the smallest $\tilde{Da}$ for which ignition is possible. The

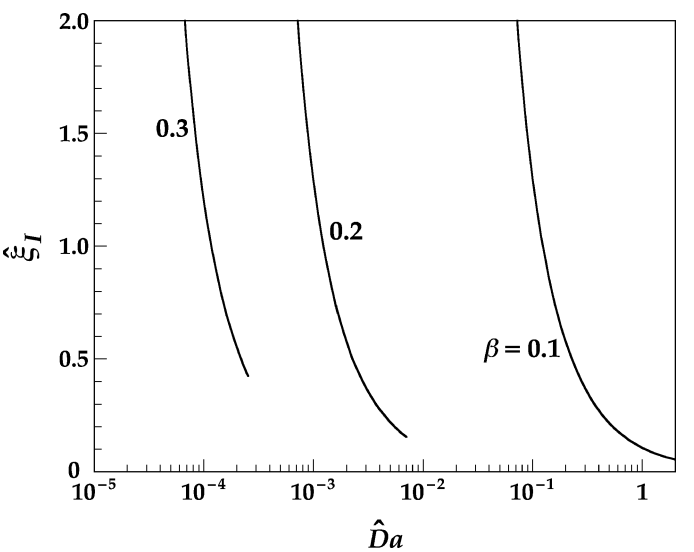

Figure 10. Rescaled plot of $\hat{\xi}_I$ versus $\hat{Da}$ from Figure 9 when changes of β is caused by variations in $\tilde{T}_0$, with $\tilde{T}_\infty = 0.00382$, $\tilde{E} = 0.127$, $\tilde{Y}_{O,\infty} = 0.0291$, and $\hat{T}_0 = 0.00673$.

minimum value of $\tilde{D}a$ below which ignition fails is then identified as the ignition state, $\tilde{D}a_I$. Ignition is successful for all $\tilde{D}a > \tilde{D}a_I$.

Figures 8 and 9 also indicate that a decrease in β for any fixed $\tilde{D}a$ favors ignition, as ignition occurs at a lower temperature increase, $\theta_{\max}$, and at a shorter ignition location, ξ_I. More importantly, a decrease in β permits ignition at a lower value of $\tilde{D}a$. Such a decrease can be accomplished either by increasing the ambient temperature, $\tilde{T}_\infty$ or q_F/c_p. Both findings are physically realistic as in the cold jet scenario.

Parameter β also can be changed by variations of the jet temperature, $\tilde{T}_0$, or the reactant mass fraction in the oxidizer supply, $\tilde{Y}_{O,\infty}$, but these changes result in a simultaneous change of $\tilde{D}a$. To investigate the effects variations in $\tilde{T}_0$ at fixed $\tilde{D}a$ requires a rescaling similar to that performed in Section 3.1. The rescaling is performed here by specifying a reference value of $\tilde{T}_0$ as $\hat{T}_0$, defining rescaled parameters $\hat{\varepsilon} = \hat{T}_0^2/\tilde{E}$, $\hat{\xi}_I = (\tilde{T}_0/\hat{T}_0)^2\,\xi_I$ and

$$\hat{D}a = \hat{\varepsilon}\,[Da\,\tilde{Y}_{F,0}/(\hat{T}_0\,\tilde{Y}_{O,\infty})]\,\exp(-\tilde{E}/\hat{T}_0), \tag{45}$$

and plotting the results in terms of rescaled variables $\hat{\xi}_I$ and $\hat{D}a$ corresponding to Figure 9. In the following discussion, $\tilde{T}_\infty = 0.00382$, $\tilde{E} = 0.127$, $\tilde{Y}_{O,\infty} = 0.0291$ and $\hat{T}_0 = 0.00673$ have been used to predict the ignition characteristics. For hydrogen, these correspond to $T_\infty = 300$ K, $E = 10\,000$ K, $Y_{O,\infty} = 0.233$, and $T_{0,\text{ref}} = 530$ K ($\beta_{\text{ref}} = 0.1$). The results are shown in Figure 10. Here an increase in $\tilde{T}_0$, which increases β without changing $\hat{D}a$, is seen to favor ignition because ignition can occur at a lower reaction rate, or lower $\hat{D}a$, as expected and in agreement with Figure 4. A plot corresponding to Figure 8 also can be performed but will not be included because the results are qualitatively similar to Figure 10.

As for the cold jet scenario, when the variation of β is caused by the change of $\tilde{Y}_{O,\infty}$, a rescaling of $\tilde{D}a$ by defining a reference value of $\tilde{Y}_{O,\infty}$, similar to that of Equation (45), is needed. The results are qualitatively the same as those presented in Figures 8 and 9 because an increase in $\tilde{Y}_{O,\infty}$ (a decrease in β) results in a greater oxidizer concentration in the reaction region.

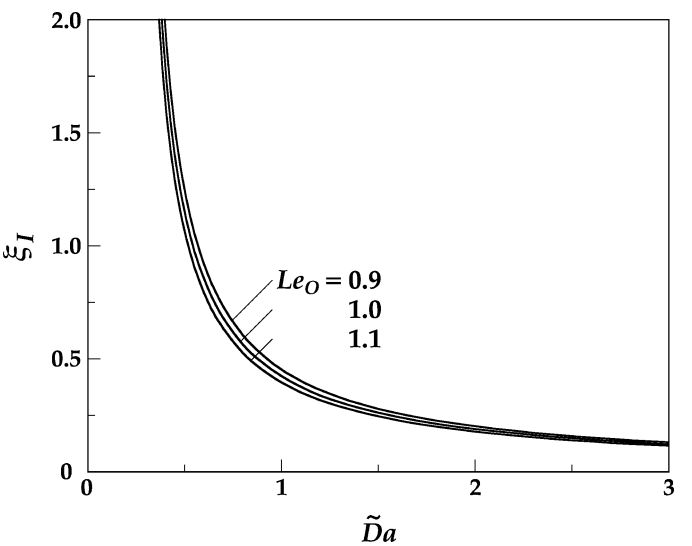

Figure 11. Effect of Le_O on ignition for a hot jet flowing into cool ambient is exhibited by plotting the ignition location ξ_I versus reduced Damköhler number $\tilde{D}a$ with $\beta = 0.3$.

The effects of oxidizer Lewis number on spontaneous ignition are considered in Figure 11 by plotting ξ_I versus $\tilde{D}a$ for various Le_O. This plot shows that a decrease in Le_O makes ignition more difficult. For an increase in the mass diffusivity of the oxidizer (or a decreased Le_O) at a fixed value of $\tilde{D}a$, ξ_I (and $\theta_{\max}$) increases. In addition, the minimum $\tilde{D}a$ for ignition increases with decreased Le_O such that a higher reaction intensity is necessary to ignite the reactants. This is contrary to the ignition behavior with respect to fuel Lewis number in the cool jet case (Figure 4). In a cool jet, there is unlimited heat transfer from the hot ambient gas to preheat the fuel so that a higher fuel diffusion rate (lower Le_F) results in a higher fuel concentration in the reaction region, more heat generation through the reaction and, hence, easier ignition. In the hot jet, only limited heat is available from the fuel flow. An increased oxidizer mass diffusivity (lower Le_O) increases the transport rate of oxidizer to the center of the jet, thus requiring more heat to preheat the oxidizer, decreasing the temperature in the hot zone, and making ignition more difficult. In addition, unlike the cool jet for which Le_F has a significant effect on ignition, the Lewis number of the oxidizer only has a weak effect on the ignition state (see Figure 11) because ignition occurs near the exit plane, if successful. In the reaction region, the flow velocity is high such that streamwise convection dominates over transverse diffusion. This observation, when combined with the fact that Le_O is close to unity for oxygen in air, indicates that the effect of Le_O in a hot-hydrogen cold-air system is secondary.

The ignition states for the hot jet scenario are shown in Figure 12 by plotting the reduced Damköhler number at ignition, $\tilde{D}a_I$, versus β when the variation of β is through the change of $\tilde{T}_\infty$, for $Le_O = 1$. Because the effect of Le_O is known from Figure 11 and is less important, it is not included in Figure 12. Instead, the effect of the oxidizer reaction order, n_O, which is obtained by replacing the $\tilde{Y}_O$ in the reaction term of Equations (11)–(13) with $\tilde{Y}_O^{n_O}$, is studied.

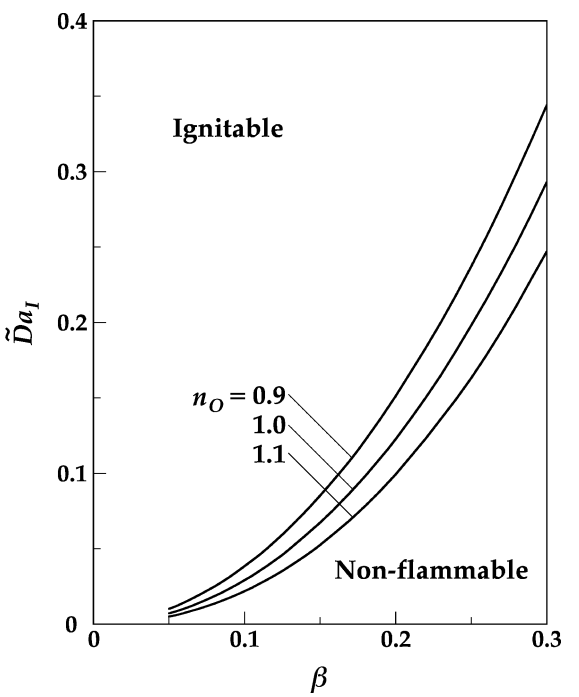

Figure 12. Variation of the ignition state, $\tilde{D}a_I$, versus β (which is changed by variations in $\tilde{T}_\infty$) for selected values of the oxidizer reaction order, n_O, hot jet flowing into cool ambient.

The region above the curve for any n_O is the region in which ignition is successful, and a flame can be established, while the region below the curve is the region where ignition fails. The plot shows that ignition is favored when β is decreased since $\tilde{D}a_I$ is reduced, in agreement with that discussed in Figure 5. Figure 12 also shows that ignition is favored when the oxidizer reaction order is increased, as the region that is ignitable is broadened. This is a result of increased reaction rate, or the heat generation rate. For cases when the variation of β is caused by the change of $\tilde{T}_0$, rescaling can be performed using Equation (45) as in Figure 10 and the result is qualitatively similar to Figure 6.

For both the cool and hot jet scenarios, the dependence of ignition on the slot width, h, can be identified through the x_0/u_0 term given in the definition of Da after Equation (16), where x_0 is given in Equation (10). Equation (10) indicates that x_0 increases with h, but the exact expression requires knowledge of the flow field in the slot. It can be shown that for a choked uniform flow driven by a high pressure gradient, and a fully-developed parabolic flow induced by a lower pressure gradient, x_0/u_0 (and all different forms of reduced Damköhler number) is proportional to h^2. Thus an increase in slot width favors ignition because there is more fuel in the jet.

4. Conclusions

The spontaneous ignition of a fuel jet, with emphasis on a hydrogen jet, emanating from a slot into an oxidizing ambient has been considered analytically. A similarity solution of the flowfield was obtained, which was then applied to the species and energy conservation equations. Solutions of the ignition conditions were found using activation energy asymptotics. Because spontaneous ignition is very sensitive to temperature, ignition is expected to occur near the edge of the jet if the fuel is cooler than the ambient gas, and on the centerline if the fuel is hotter than the ambient gas.

For a cool jet flowing into a hot ambient, ignition is found to be a strong function of ambient temperature, initial fuel concentration and fuel Lewis number, but a weak function of the reaction order of the fuel. Ignition was favored by an increase in ambient temperature and initial fuel concentration or a decrease in Lewis number. For the hot jet scenario, ignition was significantly affected by the jet temperature, moderately affected by the reaction order of the oxidizer, but only weakly affected by the oxidizer Lewis number.

The value of the mixture fraction Z at which ignition occurs can be extracted from the solutions as $Z = (\sigma Y_F - Y_O + Y_{O,\infty})/(\sigma Y_{F,0} + Y_{O,\infty})$. In the first scenario of cool jet flowing into a hot ambient, ignition occurs at $Z \to 0$ since it occurs at the jet edge where $Y_O \to Y_{O,\infty}$ and $Y_F \to 0$. In the second scenario of the hot jet, ignition occurs at the jet centerline, where $Z \to 1$ since $Y_O \to 0$ and $Y_F \to Y_{F,0}$.

The present model can be extended to studies of flame extinction and to circular jet configurations. When experimental data becomes available, parametric comparisons can be made to establish reaction rates for use in the present model.

Acknowledgment

This work was supported by NIST grant 60NANB5D1209 under the technical management of Dr. J. Yang.

References

[1] J.M. Kuchta, *Investigation of fire and explosion accidents in the chemical, mining, and fuel-related industries—a manual,* U.S. Bureau of Mines, Bulletin 680 (1985).

[2] J. Hord, *Is hydrogen a safe fuel?,* International Journal of Hydrogen Energy 3 (1978), 157–176.

[3] A.M. Kanury, *Introduction to Combustion Phenomena* (Amsterdam: Gordon and Breach Publishers) (1975).
[4] X.L. Zheng, and C.K. Law, *Ignition of premixed hydrogen/air by heated counterflow under reduced and elevated pressures,* Combustion and Flame 136 (2004), 168–179.
[5] C.E. Grosch, and T.L. Jackson, *Ignition and structure of a laminar diffusion flame in a compressible mixing layer with finite rate chemistry,* Physics of Fluids A 3 (1991), 3087–3097.
[6] H.G. Im, S.R. Lee, and C.K. Law, *Ignition in the supersonic hydrogen/air mixing layer with reduced reaction mechanisms,* Paper No. AIAA-1994-548, 32nd Aerospace Sciences Meeting and Exhibit, Reno, NV, (1994), 10–13 January.
[7] H.G. Im, B.H. Chao, J.K. Bechtold, and C.K. Law, *Analysis of thermal ignition in the supersonic mixing layer,* AIAA Journal 32 (1994), 341–349.
[8] S.R. Lee, and S.H. Chung, *On the structure of hydrogen diffusion flames with reduced kinetic mechanisms,* Combustion Science and Technology 96 (1994), 247–277.
[9] B.T. Helenbrook, and C.K. Law, *Ignition of hydrogen and oxygen in counterflow at high pressures,* Proceedings of Combustion Institute 26 (1996), 815–822.
[10] H.G. Im, B.T. Helenbrook, S.R. Lee, and C.K. Law, *Ignition in the supersonic hydrogen/air mixing layer with reduced reaction mechanisms,* Journal of Fluid Mechanics 322 (1996), 275–296.
[11] V.V. Toro, A.V. Mokhov, H.B. Levinsky, and M.D. Smooke, *Combined experimental and computational study of laminar, axisymmetric hydrogen–air diffusion flames,* Proceedings of Combustion Institute 30 (2005), 485–492.
[12] M. Chaos, R.-H. Chen, E.J. Welle, and W.L. Roberts, *Fuel Lewis number effects in unsteady Burke Schumann hydrogen flames,* Combustion Science and Technology 177 (2005), 75–88.
[13] Y. Liu, and P. Pei, *Asymptotic analysis on autoignition and explosion limits of hydrogen–oxygen mixtures in homogeneous systems,* International Journal of Hydrogen Energy 31 (2006), 639–647.
[14] F.L. Dryer, M. Chao, Z. Zhao, J.N. Stein, J.Y. Alpert, and C.J. Homer, *Spontaneous ignition of pressurized releases of hydrogen and natural gas into air,* Combustion Science and Technology 179 (2007), 663–694.
[15] F.A. Williams, *Combustion Theory*, 2nd Edition (Redwood City: Addison-Wesley) (1985).
[16] C.K. Law, *Combustion Physics* (New York: Cambridge University Press) (2006).
[17] N. Peters, *Turbulent Combustion*, (Cambridge: Cambridge University Press) (2000).
[18] A. Liñán, and F.A. Williams, *Fundamental Aspects of Combustion*, Vol. 34 of Oxford Engineering Science Series (New York: Oxford University Press) (1993).
[19] W. Bickey, *The plane jet,* Philosophical Magazine Series 7, 23 (1939), pp. 727–731.
[20] H. Schlichting, *Boundary-Layer Theory*, 7th Edition (New York: McGraw-Hill) (1979).
[21] V. Nayagam, and F.A. Williams, *Lewis-number effects on edge-flame propagation,* Journal of Fluid Mechanics 458 (2002), 219–228.